

NASA TM X-56023

DRAG REDUCTION OBTAINED BY ROUNDING VERTICAL CORNERS
ON A BOX-SHAPED GROUND VEHICLE

Edwin J. Saltzman and Robert R. Meyer, Jr.

March 1974

NASA high-number Technical Memorandums are issued to provide rapid transmittal of technical information from the researcher to the user. As such, they are not subject to the usual NASA review process.

NASA FLIGHT RESEARCH CENTER
Edwards, California 93523

DRAG REDUCTION OBTAINED BY ROUNDING VERTICAL CORNERS
ON A BOX-SHAPED GROUND VEHICLE

Edwin J. Saltzman and Robert R. Meyer, Jr.
Flight Research Center

ABSTRACT

A box-shaped ground vehicle was used to simulate the aerodynamic drag of delivery vans, trucks, and motor homes. A coast-down method was used to define the drag of this vehicle in a configuration with all square corners and a modified configuration with the four vertical corners rounded. The tests ranged in velocity from 30 miles per hour to 65 miles per hour, and Reynolds numbers ranged from 4.4×10^6 to 1.0×10^7 based on vehicle length. The modified configuration showed a reduction in aerodynamic drag of about 40 percent as compared to the square-cornered configuration.

INTRODUCTION

Many trucks, motor homes, and delivery vans are nearly box-like in configuration, having little or no rounding of the corners to reduce aerodynamic drag. It has long been known that proper shaping of vehicles, particularly at the ends, would decrease the fluid dynamic drag. The earliest boat and barge builders were aware of this fact long before ground vehicles moved fast enough to develop significant aerodynamic drag. It has only been in the last two or three decades that ground vehicles, especially those designed for high volumetric efficiency, have traveled fast enough for aerodynamics to be an important drag factor.

During the era of inexpensive gasoline and diesel fuel, the problem of aerodynamic drag for trucks was accommodated primarily by resorting to more powerful engines. However, recent rising fuel prices and the uncertainty of fuel reserves for future needs have caused increased concern about the efficiency of all kinds of powered vehicles.

For box-like vehicles an obvious way to reduce the drag is to round the corners, though there are certainly other methods which should be effective. Though this method is well known and the results have been measured on models, many

manufacturers of such vehicles have not used rounded corners. Whether this is because of (a) extra fabrication costs, (b) loss of volumetric efficiency, or (c) uncertainty about the potential benefits is not known. A listing of investigations involving the determination of ground vehicle drag, the estimation of drag, and various means of reducing ground vehicle drag would include references 1 to 8.

Obviously, there is now much greater concern about fuel consumption, and perhaps designers will want to consider incorporating some simple volume-drag trade-offs or add-on devices if the drag reduction is large enough. Thus the NASA Flight Research Center began construction of a representative vehicle during the summer of 1973 and started tests on the vehicle in the fall of 1973. This paper presents drag results from the box-shaped vehicle before and after the four vertical corners were rounded. A simple coast-down technique was used to define the drag.

SYMBOLS

A	body cross-sectional area (same for both configurations)
C_{D_a}	aerodynamic drag coefficient, D_a/qA
D	drag
g	local acceleration of gravity
q	dynamic pressure, $\frac{1}{2}\rho V_c^2$
r	radius of rounded vertical corners
Δt	time increment
V	velocity
ΔV	velocity increment
W	vehicle weight during each test
w	vehicle width
ρ	air density

Subscripts:

a	aerodynamic
c	calibrated

m mechanical¹
t total

TEST VEHICLE AND METHOD

The box shape of the test vehicle was obtained by modifying an ordinary commercial cab-over-engine van (fig. 1). Baseline drag data were obtained with this carrier vehicle to determine the potential quality of the data which could be obtained without an exotic data system. These drag data were obtained by converting the coasting deceleration into total drag, i.e., the sum of the aerodynamic and mechanical¹ drag:

$$D_t = D_m + D_a = \frac{\Delta V}{\Delta t} \frac{W}{g}$$

A more complex approach to the coast-down method can be found in reference 9; however, the present relatively straightforward approach is adequate for the purposes of this report and for the conditions of the tests, in that test conditions were carefully controlled to maintain constant mechanical drag, within narrow limits, for every test and each configuration at a given speed. Thus changes in configuration produced drag changes which were aerodynamic in origin.

With this approach in mind, it was decided to add an easily predictable increment of drag to the carrier vehicle and compare the measured increment with the prediction. If this comparison showed good correlation, it was planned to construct a box-like configuration over the vehicle.

The configuration with the added drag increment (flat plate and supporting structure) is shown in figure 3. The measured increment and the predicted increment of "drag" are shown in figure 4. The predicted curve is based on information from reference 4, chapter 3. These results were converted to an increment of horsepower because, at this stage in the experiment, the decision to continue or discontinue the study was contingent upon our ability to discriminate to within 2 horsepower. The agreement between the measured and the predicted values of horsepower required to overcome the added drag was encouraging. Thus it was decided to modify the carrier vehicle to a box shape.

The carrier vehicle was fitted with an aluminum subframe as shown in figure 5. A maximum radius for the vertical corners of 16 inches was anticipated, so this was built into the framework. The subframe was covered with aluminum sheet having

¹The van had a manual, three-speed transmission which was set in neutral during each deceleration run. Thus the mechanical drag consists of (1) tractive drag of the tires and bearings and the gear resistance back through the drive line to the transmission (fig. 2) and (2) thrust from the rotational inertia of the wheels and tires.

a maximum gage of 0.032 inch and a minimum of 0.020 inch at the vertical corners. Formers at the vertical corners permitted the attachment of the square corners for the basic box shape. The finished vehicle (square corners) is shown in figure 6(a) with the engine cooling vent open. Similar views of the vehicle with rounded vertical corners and the cooling vent closed are shown in figure 6(b). The door for this vent was closed for all the deceleration test results presented in this report.

The engine cooling air was channeled directly to the radiator when the vent door was open, i.e., the channel was sealed where appropriate so that all the air entering the open door passed through the radiator. Figure 5 shows how this was done and also shows the sheet metal seal between the bottom member of the subframe and the front bumper. The wheel wells and lower-aft subframe were similarly sealed with sheet metal and taped as necessary to insure that there was no air flow between the carrier vehicle and the box.

Plexiglas sheets were used to provide the somewhat limited visibility. Other non-highway characteristics were the absence of exterior rear view mirrors, head and tail lights, windshield wipers, and turn signals. Thus the vehicle was towed, rather than driven, over the roads of Edwards Air Force Base to the test site.

The dimensions of the test vehicle in the square-cornered configuration are shown in figure 7. The corner radius for the configuration with rounded vertical corners was 16 inches, which corresponded to a r/w (radius divided by vehicle width) ratio of 0.2. This radius was chosen as a reasonable conservative upper limit for a three-dimensional system in the presence of the ground, based on the data and comments compiled in reference 4. It is realized, also on the basis of reference 4, that the optimum r/w ratio is probably between 0.2 and 0.1 (considering the conflicting needs for reduced drag and maximum volume for a given vehicle length).

INSTRUMENTATION AND TEST CONDITIONS

The deceleration of the test vehicle was determined in two ways during a test. In the primary method a calibrated speedometer and a bank of six 1/10-second stopwatches were used. In the backup method an accelerometer of $\pm 0.1g$ range was combined with a recording oscillograph. The end points of six specific velocity increments were called off the calibrated speedometer. These velocity increments were each assigned an interval of time as provided by the bank of watches shown in figure 8. All watches were started at the beginning of the first interval. Then, one by one, each watch was stopped as each velocity increment ended.

The accelerometer, of course, provided in a more direct manner a continuous record of deceleration. One channel of the oscillograph was assigned as an event marker so that specific velocities could be identified and correlated with the corresponding deceleration values.

The tests were made on an auxiliary runway at Edwards Air Force Base, Calif. The runway had an exceptionally smooth asphalt surface and a constant elevation

gradient of only 0.08 percent, thus the gradient effects on deceleration were small and were eliminated by averaging successive runs in opposite directions. The tests were performed early in the day when winds were calm or nearly calm; testing was canceled when winds exceeded 2 or 3 knots. Because successive tests made in opposite directions were averaged, the effects of such low winds are believed to be negligible; nevertheless, most tests were made under calm conditions.

In addition to the wind velocity and direction, ambient pressure and temperature were documented continually during each day's testing. Data system battery voltages were also monitored, and regular, closely spaced tare readings were made on the accelerometer-recorder system so that any tendency to drift could be accounted for.

The methods and instrumentation used and the conditions under which the tests were made provided drag measurements that were consistent from method to method and day to day.

RESULTS

Drag results obtained from tests of the configuration with square corners and the configuration with rounded vertical corners are shown in figure 9. These data represent an average of 14 tests for the square-cornered configuration and 20 tests for the rounded configuration. The data shown were obtained from stop-watch-speedometer readings, and thus define the total drag of the two configurations in an absolute sense. Reynolds numbers based on the vehicle length ranged from 4.4×10^6 to 1.0×10^7 for the velocity range of these data. The symbol at $V \rightarrow 0$ is the low-limit tractive drag obtained for the vehicle for the test tire pressures on the surface of the test runway. This tractive drag was obtained with a fish-type scale of 100 pound range. The vehicle was towed at approximately 2 miles per hour during this measurement. The dashed curve is an extrapolation of the measured low-limit tractive drag based on the semiempirical equation from Hoerner (ref. 4, ch. 12).

At 55 miles per hour, the configuration with the rounded corners has a drag level similar to that of the square-cornered vehicle at approximately 44 miles per hour. Conversely, extrapolation of the modified (rounded) vehicle results to higher speeds shows that at approximately 70 miles per hour the more refined configuration would have about the same drag as the square-cornered vehicle at 55 miles per hour.

The test van front suspension, though stiffened by auxiliary helper springs, was flexible enough to allow some depression of the front of the vehicle during deceleration. Thus the accelerometer sensed the effect of the lowered front of the vehicle, a component of the acceleration of gravity, in addition to the rate of change of forward velocity. Thus the apparent drag, based on the accelerometer output, was too large for both of the test configurations. Nevertheless, the difference in drag between the two configurations, as defined by the accelerometer, is an authentic backup measurement and confirms the results obtained from the primary stop-watch-speedometer method. The incremental drag differences determined by both

methods are shown in the following table in terms of the reduction in drag as a percentage of the total drag for the square-cornered configuration:

V _c , miles/hour	Drag reduction D _t (square corners), percent	
	Speedometer- stopwatch method (primary)	Accelerometer method (backup)
30	22	20
40	25	28
50	29	31
60	33	29

The decrease in drag, which is aerodynamic in origin, can also be considered as a percentage of the aerodynamic component of drag of the square-cornered vehicle instead of as a percentage of the total drag (i.e., as a percentage of the measured total drag minus the mechanical drag). On the latter basis the drag reduction provided by the rounded vertical corners, as defined by the speedometer-stopwatch method, would be about 40 percent at 60 miles per hour. This reduction in drag was achieved by sacrificing 1.4 percent in vehicle volume.

Subtracting the extrapolated tractive drag from the total drag and accounting for the thrust from the rotational inertia of wheels and tires also permits an aerodynamic drag coefficient, C_{D_a} , to be calculated for each configuration. Based on an area of 35.3 square feet, which is the body cross-sectional area, the aerodynamic drag coefficient is 1.13 for the square-cornered configuration and 0.68 for the modified configuration. The value of 1.13 is significantly higher than the drag coefficient (0.86) shown in reference 4 for a square-cornered vehicle tested in a wind tunnel. If reference 4 used the box projected frontal area plus the exposed wheel projected area as the reference, about one-fourth of the difference could be accounted for. It is suspected that the higher drag coefficient values calculated for the square-cornered vehicle of the present study are caused primarily by the unsealed underbody which would not have been simulated by the model reported in reference 4.

The present study was limited to the coast-down method of sensing drag, which does not define relative gas consumption, or gas mileage, per se for the respective configurations. Thus the drag reduction which has been demonstrated

will not be interpreted quantitatively in terms of potential savings in fuel. However, references 3, 10, and other studies do suggest that a qualitative statement can be made in this regard. On this basis, then, potential fuel savings, in percent, would be between one-third to one-half the magnitude of the percentage decrease in aerodynamic drag, obviously depending on the particular vehicle, the routing, the type of driving, winds, and other factors.

Tuft photographs were made during tests of the two configurations over a range of velocities and with the cooling vent open and closed. The pictures provide a graphic explanation of the significant differences in drag. Figures 10(a) and 10(b) show results that are typical of the entire highway speed range. It is obvious that the square-cornered configuration (fig. 10(a)) has separated flow just behind the front corner and reverse flow, of sorts, from somewhere near the middle of the vehicle side to ahead of the front wheels. Only the aft one-third to one-half of the side shows the beginnings of attached flow. The configuration with rounded vertical corners (fig. 10(b)) has attached flow along the side throughout the regions shown by the photograph, back to some portion of the rear rounded corner. Tuft photographs with the cooling vent open showed the same patterns as with the vent closed except for the region immediately adjacent to the opening.

All of the drag data presented were from tests with the cooling vent closed. Decelerations were made with the vent initially opened and then suddenly closed. The accelerometer data do not show a significant difference in drag between the two conditions.

SUMMARY

A box-shaped vehicle was tested to obtain baseline drag data for square-cornered ground vehicles such as delivery vans, motor homes, and trucks. The baseline tests for the square-cornered vehicle were followed by a drag evaluation of the same vehicle with rounded vertical corners on both the front and rear. The tests covered the velocity range from 30 miles per hour to 65 miles per hour, and the Reynolds number range was from 4.4×10^6 to 1.0×10^7 , based on vehicle length.

Rounding the vertical corners of the vehicle reduced the total drag approximately 22 percent at the lower test speeds and approximately 33 percent at the higher test speeds. On the basis of the aerodynamic component of drag, the decrease in drag was about 40 percent at 60 miles per hour.

Flight Research Center

National Aeronautics and Space Administration

Edwards, Calif., March 4, 1974

REFERENCES

1. Flynn, Harold; and Kyropoulos, Peter: Truck Aerodynamics. SAE Preprint 284A, 1961.
2. Kirsch, Jeffrey W.; Garg, Sabodh K.; and Bettes, William: Drag Reduction of Bluff Vehicles With Airvanes. SAE paper 730686, 1973.
3. Ritchie, Dave: How To Beat the Built-in Headwind. Owner Operator, May/June 1973, pp. 89-99.
4. Hoerner, Sighard F.: Fluid-Dynamic Drag. Pub. by the author (148 Busted Dr., Midland Park, N.J.), 1965.
5. Larrabee, E. Eugene: Small Scale Research in Automobile Aerodynamics. SAE paper 660384, 1966.
6. Gross, Donald S.; and Sekscienski, William S.: Some Problems Concerning Wind Tunnel Testing of Automotive Vehicles. SAE paper 660385, 1966.
7. White, R. G. S.: A Method of Estimating Automobile Drag Coefficients. SAE paper 690189, 1969.
8. Turner, Thomas R.: Wind-Tunnel Investigation of a 3/8-Scale Automobile Model Over A Moving-Belt Ground Plane. NASA TN D-4229, 1967.
9. White, R. A.; and Korst, H. H.: The Determination of Vehicle Drag Contributions from Coast-Down Tests. SAE paper 720099, 1972.
10. Austin, Thomas C.; and Hellman, Karl H.: Passenger Car Fuel Economy - Trends and Influencing Factors. SAE paper 730790, 1973.

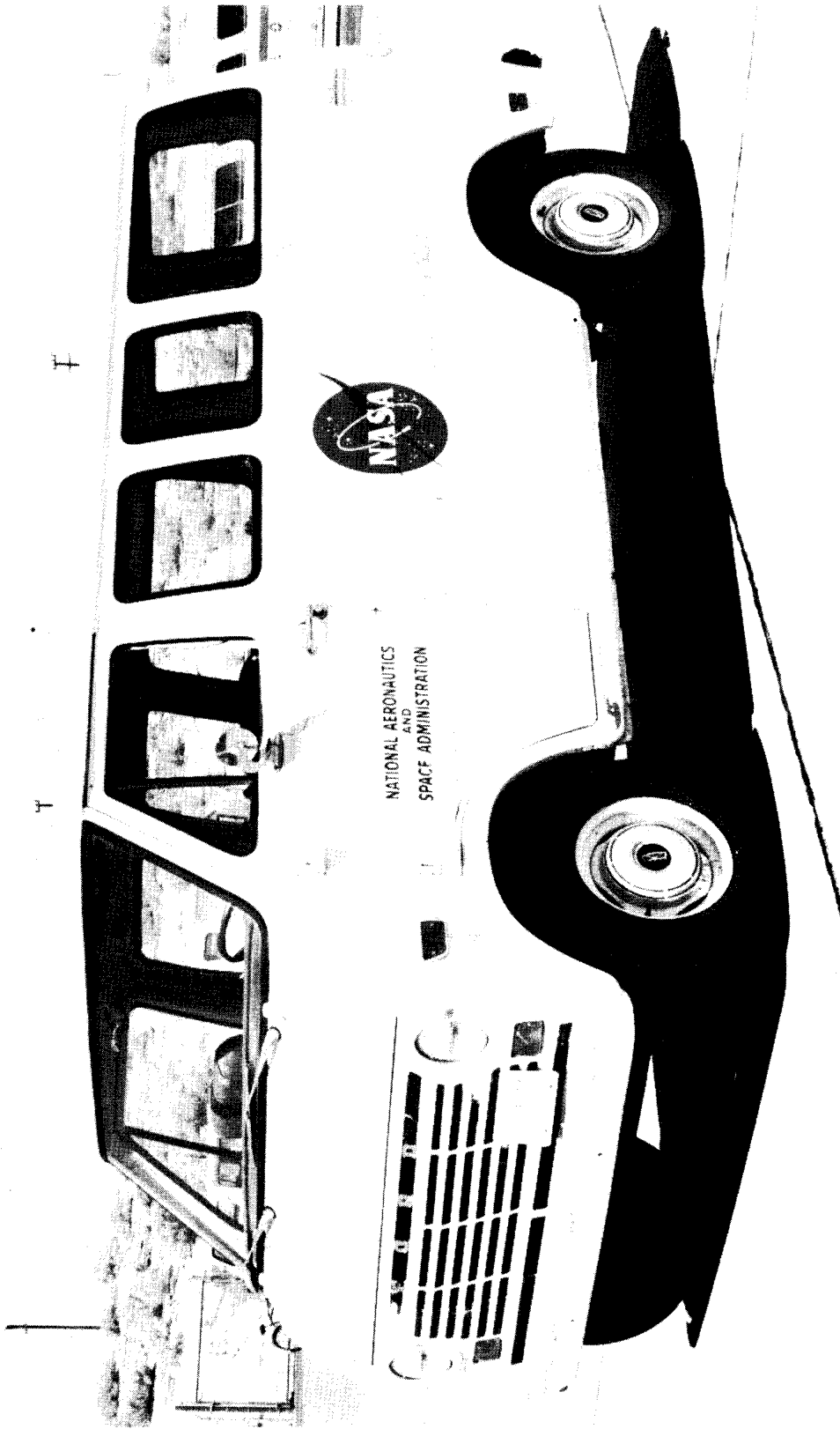


Figure 1. Carrier vehicle.

E-26449

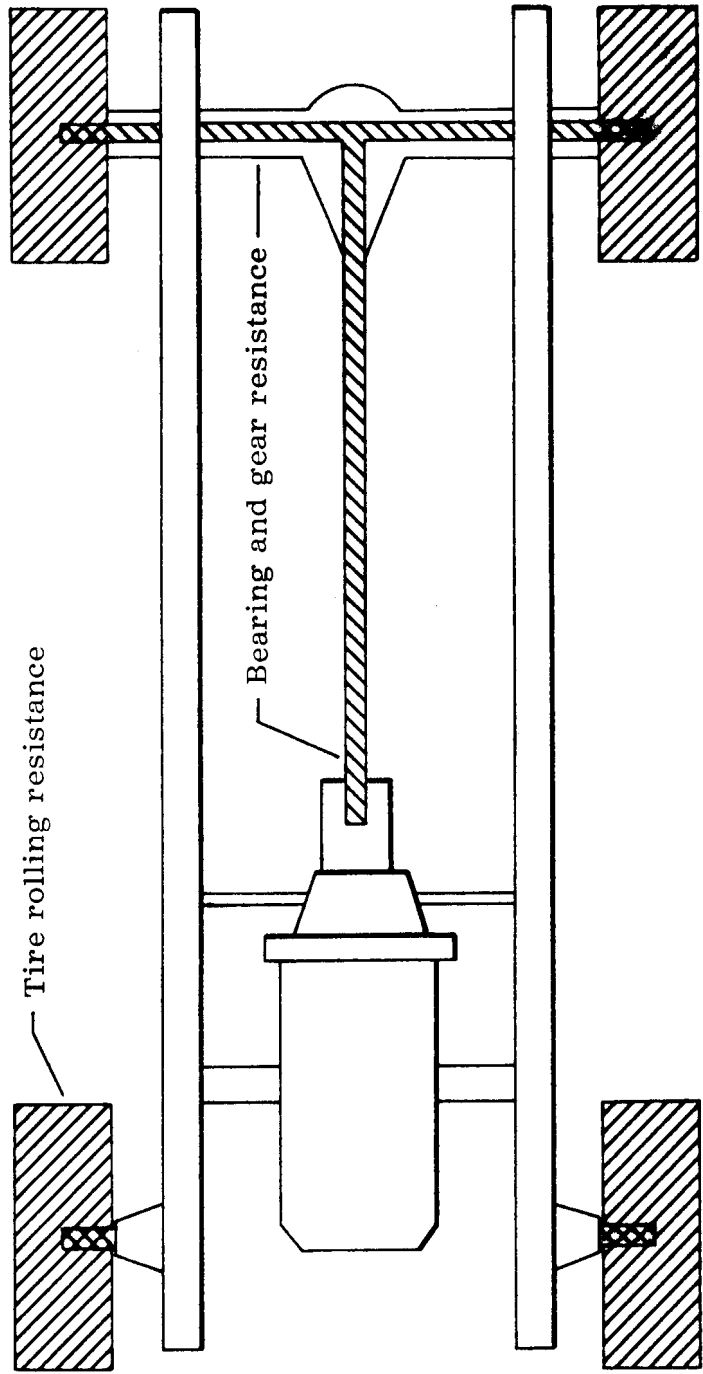


Figure 2. Schematic showing sources of tractive drag.

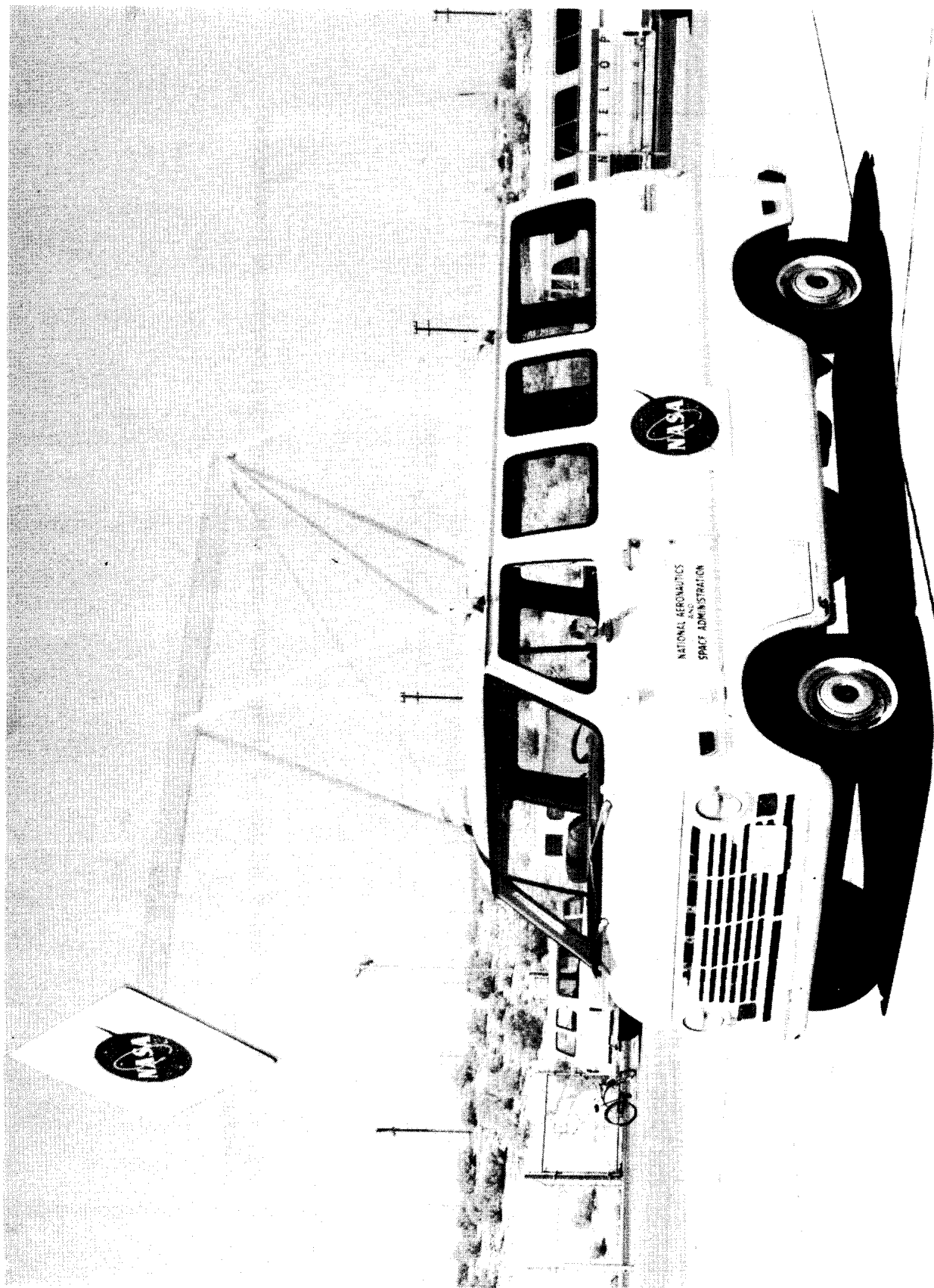
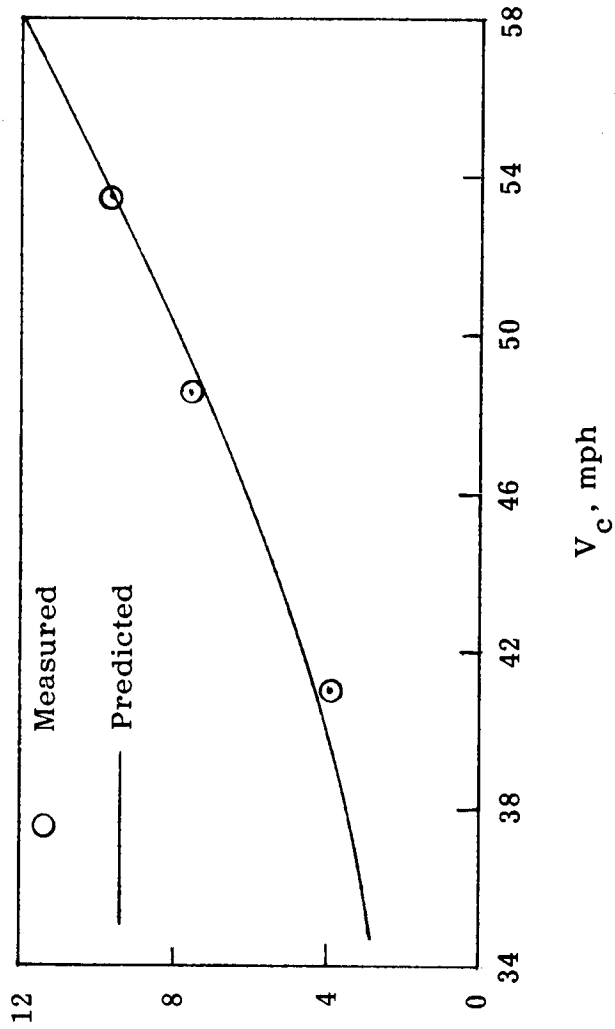


Figure 3. Carrier vehicle with flat plate and supporting structure.

E-26454



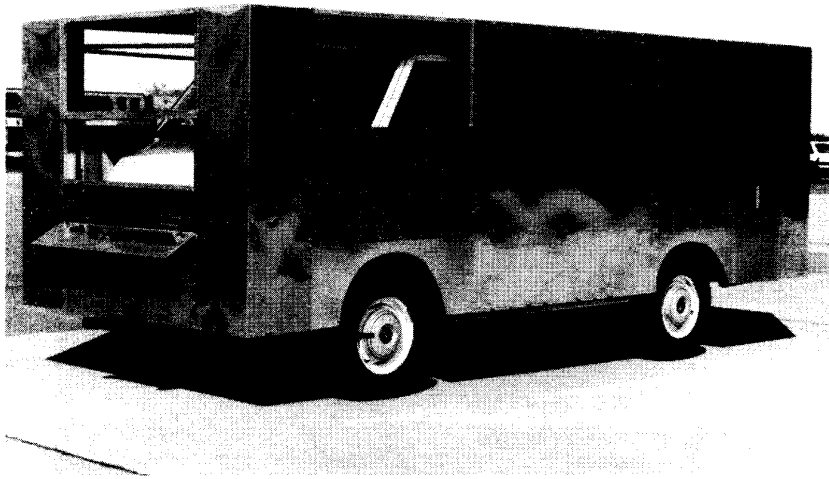
Horsepower increment,
 (horsepower of van +
 supporting structure +
 flat plate) - (horsepower
 of van)

Figure 4. Comparison of measured "drag" increment with predicted increment (converted to horsepower).

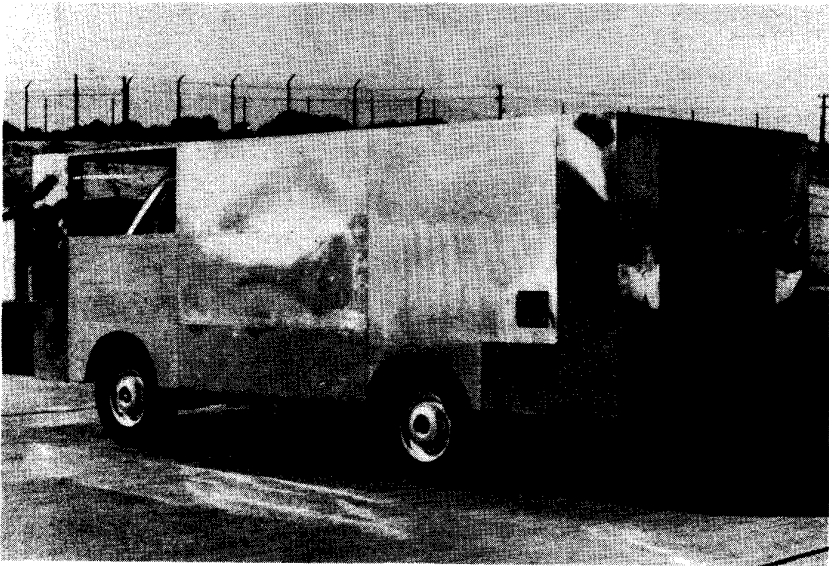


E-26477

Figure 5. Carrier vehicle with aluminum subframe.



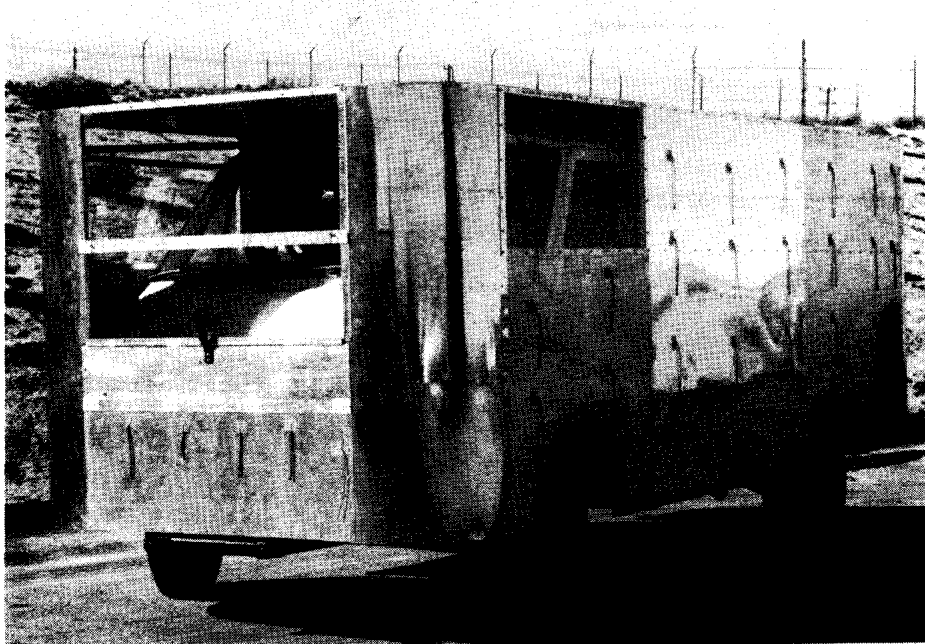
E-26577



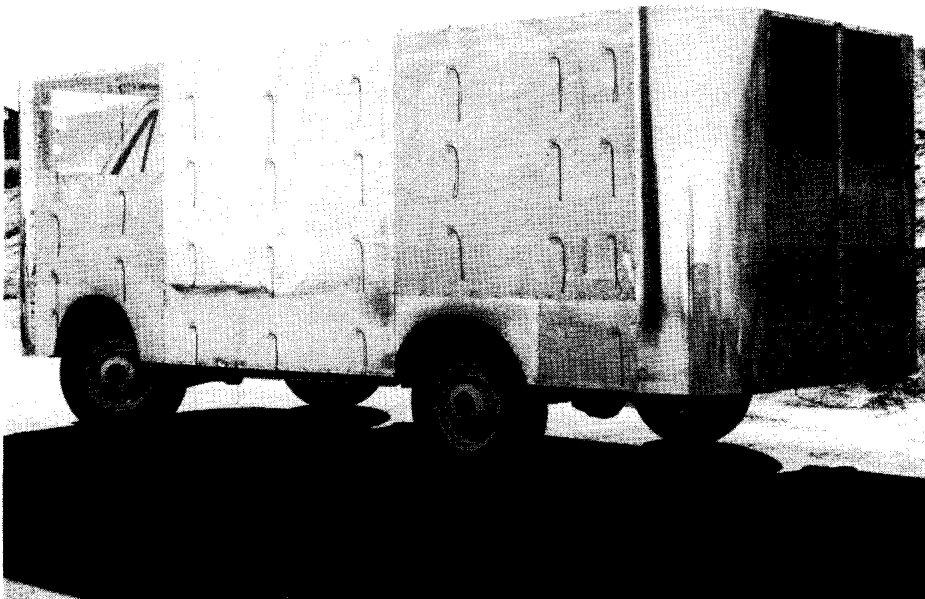
E-26575

(a) Configuration with square corners; cooling vent open.

Figure 6. Test vehicle.



E-26776



E-26774

(b) Configuration with rounded vertical corners, front and rear; cooling vent closed.

Figure 6. Concluded.

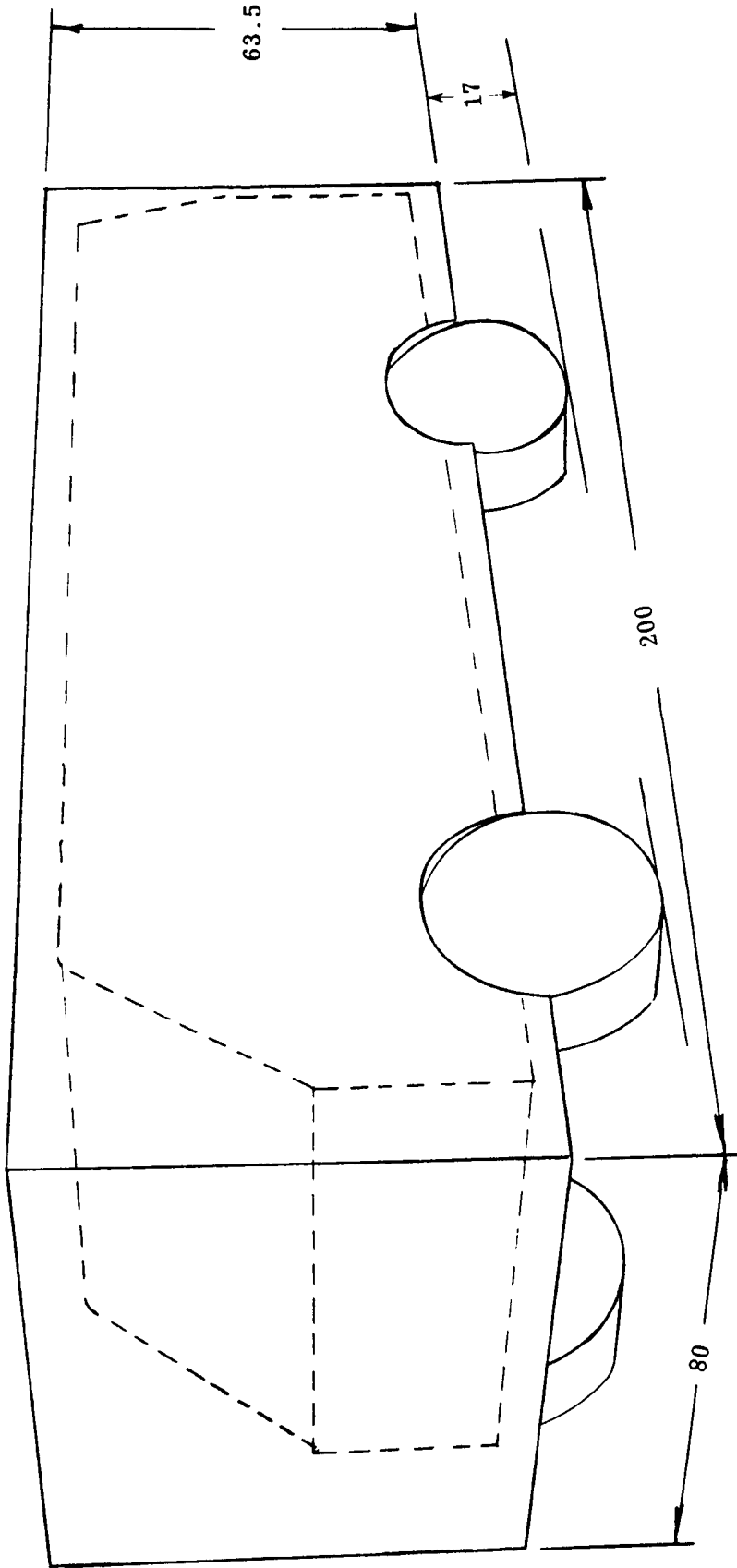


Figure 7. Sketch of test vehicle showing dimensions (in inches) for the square-cornered configuration.

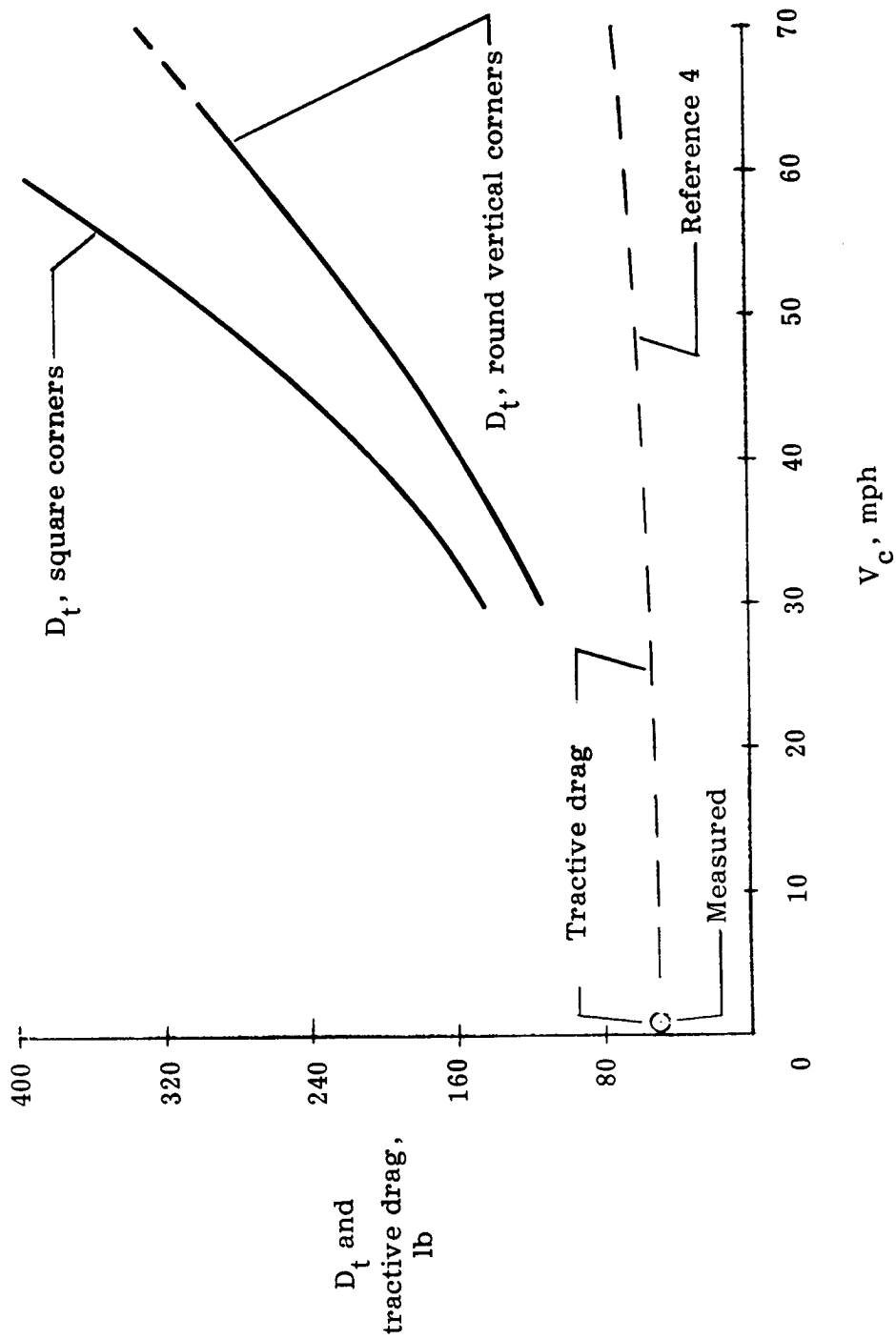
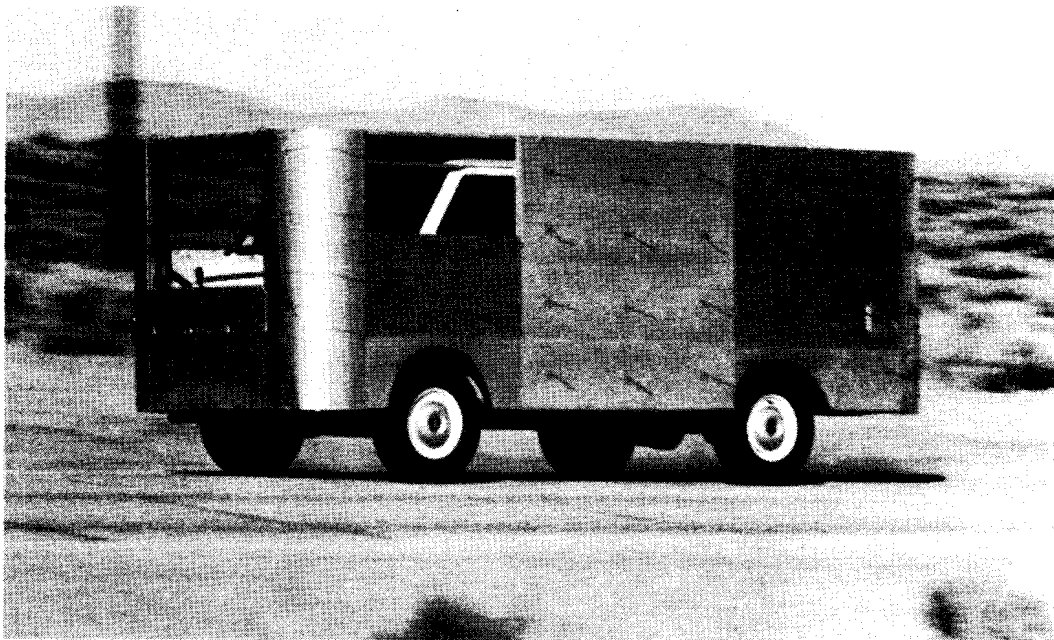


Figure 9. Relationship of total drag to velocity obtained by the coast-down method with stopwatch-speedometer readings. (The tractive drag does not include the rotational inertia of wheels and tires.)



(a) Square corners.

E-26717



(b) Rounded vertical corners.

E-26903

Figure 10. Tuft patterns for each configuration at a calibrated speed of 55 miles per hour with the cooling vent closed.